

# Chandra observations of SGR 1627–41 near quiescence

Hongjun An<sup>1</sup>, Victoria M. Kaspi<sup>1,2</sup>, John A. Tomsick<sup>3</sup>, Andrew Cumming<sup>1</sup>, Arash Bodaghee<sup>3</sup>, Eric Gotthelf<sup>4</sup> and Farid Rahoui<sup>5</sup>

## ABSTRACT

We report on an observation of SGR 1627–41 made with the *Chandra X-ray Observatory* on 2011 June 16. Approximately three years after its outburst activity in 2008, the source’s flux has been declining, as it approaches its quiescent state. For an assumed power-law spectrum, we find that the absorbed 2–10 keV flux for the source is  $1.0^{+0.3}_{-0.2} \times 10^{-13}$  erg cm<sup>−2</sup> s<sup>−1</sup> with a photon index of  $2.9 \pm 0.8$  ( $N_H = 1.0 \times 10^{23}$  cm<sup>−2</sup>). This flux is approximately consistent with that measured at the same time after the source’s outburst in 1998. With measurements spanning 3 years after the 2008 outburst, we analyze the long-term flux and spectral evolution of the source. The flux evolution is well described by a double exponential with decay times of  $0.5 \pm 0.1$  and  $59 \pm 6$  days, and a thermal cooling model fit suggests that SGR 1627–41 may have a hot core ( $T_c \sim 2 \times 10^8$  K). We find no clear correlation between flux and spectral hardness as found in other magnetars. We consider the quiescent X-ray luminosities of magnetars and the subset of rotation-powered pulsars with high magnetic fields ( $B \gtrsim 10^{13}$  G) in relation to their spin-inferred surface magnetic-field strength, and find a possible trend between the two quantities.

*Subject headings:* pulsars: individual (SGR 1627–41) — stars: magnetars — stars: neutron — X-rays: bursts

---

<sup>1</sup>Department of Physics, Rutherford Physics Building, McGill University, 3600 University Street, Montreal, Quebec, H3A 2T8, Canada

<sup>2</sup>Lorne Trottier Chair; Canada Research Chair

<sup>3</sup>Space Sciences Laboratory, University of California, Berkeley, CA 94720, USA

<sup>4</sup>Columbia Astrophysics Laboratory, Columbia University, 550 West 120th Street, New York, NY 10027, USA

<sup>5</sup>Department of Astronomy & Harvard-Smithsonian Center for Astrophysics, Harvard University, 60 Garden Street, Cambridge, MA 02138, USA

## 1. Introduction

Magnetars are neutron stars with ultra-strong magnetic fields, the decay of which is theorized to power the observed radiation from the star (Thompson & Duncan 1995, 1996; Thompson et al. 2002). Soft Gamma Repeaters (SGRs) and Anomalous X-ray Pulsars (AXPs) are two observational manifestations of magnetars. The former show repeated soft gamma-ray bursting activity and have relatively hard spectra, and the latter have soft spectra typically characterized by a blackbody plus power law. However, the distinction between the two has become increasingly blurred (Thompson et al. 2002; Gavril et al. 2002; Pons et al. 2007; Perna & Pons 2011). Magnetars generically show X-ray outbursts, which are sudden increases of luminosity by orders of magnitude for days to months. During outbursts, almost all the properties of magnetars, such as their flux, spectrum and pulsed flux, change (see Woods & Thompson 2006; Kaspi 2007; Mereghetti 2008; Rea & Esposito 2011, for reviews). The X-ray luminosities of the first-discovered magnetars were typically  $\sim 10^{35}$  erg s $^{-1}$ , orders of magnitude greater than their spin-down luminosity. However, more recent discoveries of magnetars in outburst suggest most magnetars in quiescence may be far less luminous (e.g. 1E 1547.0–5408, XTE J1810–197, Swift J1822–1606; Gelfand & Gaensler 2007; Bernardini et al. 2009; Scholz et al. 2012). The spin periods of magnetars<sup>1</sup> are in the narrow range of 2–12 s and are relatively long compared to those of radio pulsars. The magnetic-field strength inferred from the spin period and spin-down rate is typically  $B > 10^{14}$  G, assuming the standard vacuum dipole formula for magnetic braking, although several with  $B \lesssim 10^{14}$  G have recently been found (Rea et al. 2010; Scholz et al. 2012; Rea et al. 2012).

The recent discoveries of a magnetar-like outburst from a high- $B$  rotation-powered pulsar (RPP) (PSR J1846–0258, Gavril et al. 2008), pulsed radio emission from a magnetar (XTE J1810–197, Camilo et al. 2006), a low magnetic field magnetar (SGR 0418–5729, Rea et al. 2010), and the very low X-ray luminosities measured for several magnetars are of particular interest. These raise important questions about the relationship between magnetars and other types of neutron stars, and why there is such an apparent diversity in magnetar properties. For example, what determines a magnetar’s quiescent X-ray luminosity? According to conventional magnetar models (Thompson & Duncan 1995, 1996; Thompson et al. 2002), there should be a correlation between  $B$  and the X-ray luminosity. However, transient magnetars, with their faint quiescent luminosities compared with non-transient magnetars of the same inferred  $B$ , challenge this. And relatedly, are high- $B$  RPPs in general magnetars in quiescence? PSR J1846–0258’s outburst suggests this, but it is only one source. Pons et al.

---

<sup>1</sup>See the online magnetar catalog for a compilation of known magnetar properties, <http://www.physics.mcgill.ca/~pulsar/magnetar/main.html>

(2007) and Perna & Pons (2011) argue that magnetars and RPPs are all related on the basis of magneto-thermal evolution theory. Also a possible connection between high- $B$  RPPs and magnetars has been suggested on the basis of possibly high thermal temperatures of high- $B$  RPP X-ray emission (Kaspi & McLaughlin 2005; Zhu et al. 2009; Olausen et al. 2010; Zhu et al. 2011; Ng & Kaspi 2011). However, it is important to study many magnetars and RPPs in quiescence to better address this question.

SGR 1627–41 was discovered on 1998 June 15 with the Burst and Transient Source Experiment (BATSE, Fishman 1989). It was then identified as a SGR by Kouveliotou et al. (1998). It is located at R.A. =  $16^{\text{h}}35^{\text{m}}51^{\text{s}}.844$ , Dec. =  $-47^{\circ}35'23''.31$  (J2000.0) and is estimated to be  $11.0 \pm 0.3$  kpc away based on an apparent association with a star-forming region and molecular cloud (Hurley et al. 1999; Corbel et al. 1999; Wachter et al. 2004). The spin period and the spin-down rate were not measured until recently due to the faint nature of the source in quiescence. After another outburst in 2008 May, the spin period and the spin-down rate were measured to be  $2.594578(6)$  s and  $1.9(4) \times 10^{-11}$  s s $^{-1}$ , which imply an inferred surface dipolar magnetic-field strength of  $B \equiv 3.2 \times 10^{19} (P\dot{P})^{1/2}$  G =  $2 \times 10^{14}$  G (Esposito et al. 2009a,b). The lowest flux ever measured for this magnetar is  $6 \times 10^{-14}$  erg cm $^{-2}$  s $^{-1}$  (2–10 keV,  $\sim 10$  years after the 1998 outburst, Esposito et al. 2008). However, whether it was in quiescence at that time is not clear; the luminosity might have declined further had the outburst not occurred in 2008.

Here, we report the results of an observation made with *Chandra* in the direction of SGR 1627–41. We then combine our flux measurement of SGR 1627–41 with previous values to determine the long-term flux evolutions after its outbursts, and attempt to fit them to a model to infer thermal properties of the source. We compare the flux we measure with that from the same time after the first outburst and the lowest flux ever measured. Finally, we compile quiescent X-ray luminosities of magnetars and high- $B$  RPPs to search for a correlation with spin-inferred  $B$ , as might be expected in the magnetar model.

## 2. Observations

SGR 1627–41 was observed with *Chandra* as part of a Norma arm survey (PI: Tomsick) on 2011 June 16. Data from SGR 1627–41 were recorded in two consecutive 19 ks exposures (IDs 12528, 12529), using the Advanced CCD Imaging Spectrometer I-array (ACIS-I, Garmire et al. 2008). The data were initially processed at the *Chandra* X-ray Center (CXC) with ASCDS Version 8.3.4. After obtaining the data from the CXC, we performed all subse-

quent processing with the CIAO 4.3.1 software<sup>2</sup>. We used the CIAO program `chandra_repro` along with CALDB 4.4.5 to produce the “level 2” event lists that we used for further analysis.

### 3. Data analysis and results

#### 3.1. Imaging Analysis

We detect the source in both exposures with `wavdetect` in CIAO. The best positions obtained are R.A. =  $16^{\text{h}}35^{\text{m}}51^{\text{s}}.882$ , Dec. =  $-47^{\circ}35'23''.35$  (J2000.0) with off-axis angle of  $7'.15$  for exposure 1 (ID 12528) and R.A. =  $16^{\text{h}}35^{\text{m}}51^{\text{s}}.786$ , Dec. =  $-47^{\circ}35'22''.35$  (J2000.0), with off-axis angle of  $7'.60$  for exposure 2 (ID 12529). On average, the position is R.A. =  $16^{\text{h}}35^{\text{m}}51^{\text{s}}.834$  and Dec. =  $-47^{\circ}35'22''.85$  (J2000.0). Using the empirical formula of Hong et al. (2005), we estimated the position uncertainties to be  $P_{\text{err}} = 1''.1$  (ID 12528) and  $P_{\text{err}} = 1''.3$  (ID 12529). Therefore, we conclude the positions measured from the two exposures are consistent with each other and with the known position of the source.

After finding the source location, we conducted an imaging simulation using *Chandra* Ray Tracer<sup>3</sup> (ChaRT) and the MARX<sup>4</sup> tool in CIAO 4.3., and comparing with our data, find that there is no extended emission with 90% confidence. We find no evidence for the diffuse emission and hard-spectrum ‘spot’ reported by Esposito et al. (2009a) on the basis of a deep *XMM-Newton* observation, although this is not unexpected due to the low brightness of the diffuse emission ( $\sim 10^{-14}$  erg cm<sup>-2</sup> s<sup>-1</sup> arcmin<sup>-2</sup>) and the relatively large angular separation of the hard-spectrum ‘spot’ ( $\sim 2'$  from the source).

#### 3.2. Timing Analysis

Since the timing resolution of ACIS-I is 3.24 s, it is not possible to measure the spin period of the source ( $\sim 2.6$  s) with this observation. However, to search for any type of aperiodic variability in the emission, we produced light curves with different binnings (2–7 bins over 38 ks, to have the average counts per bin greater than 20). We also performed the Kolmogorov-Smirnov test (KS-test) and the Gregory-Loredo test (using the `glvary` tool in CIAO) on the data with a null hypothesis that the events are drawn from a flat light curve

---

<sup>2</sup><http://cxc.harvard.edu/ciao-4.3>

<sup>3</sup><http://cxc.harvard.edu/chart/>

<sup>4</sup><http://space.mit.edu/CXC/MARX>

and find that the null hypothesis is statistically consistent with the data. Therefore, we conclude that there was no aperiodic variability in this observation over the range searched.

### 3.3. Spectral Analysis

We extracted the source counts using a radius of  $10''$  (which includes  $\sim 95\%$  energy with the spectrum given below), and the background with an annulus of inner radius  $10''$  and outer radius  $60''$  centered at the source positions reported in Section 3.1, and produced spectra using the **SPEXTRACT** tool of CIAO 4.3 with CALDB 4.4.6.1. We find  $65 \pm 8$  and  $60 \pm 8$  source counts in 2–8 keV for exposures 1 and 2, respectively. The 2–8 keV band is chosen because there is only 1 event below 2 keV in the source region for each exposure due to the large hydrogen column density ( $N_H$ ). Since there are very few counts in each exposure, we combine the spectra for the two. Even summing the spectra, we are not able to tell whether a power law or a blackbody fits the data better. Therefore, we report the results from fits with both models. We use the **wabs\*powerlaw** and the **wabs\*bbbody** models of XSPEC 12.7.0<sup>5</sup> to fit the data.

We fit the data with Churazov weighting with XSPEC because of the low count rate. In fitting, we fix  $N_H$  to the previously measured value, determined when the source was bright ( $1.0 \times 10^{23} \text{ cm}^{-2}$ , Esposito et al. 2009a). From the fit, we find the power-law index ( $\Gamma$ ) of  $2.9 \pm 0.8$  ( $kT = 0.85_{-0.16}^{+0.25}$  keV), and observed flux  $F_X = 1.0_{-0.2}^{+0.3} \times 10^{-13}$  ( $0.75_{-0.17}^{+0.20} \times 10^{-13}$  erg  $\text{cm}^{-2} \text{ s}^{-1}$ ) in the 2–10 keV band for the power law (blackbody). We present the fit results in Table 1. We also tried alternative methods to fit the data: the usual Chi-squared fit (grouping 15 counts per bin), a C-statistic fit (**CSTAT** in XSPEC, unbinned), and Chi-squared fit with Gehrels weighting (grouping 5 counts per bin), and obtained consistent results.

### 3.4. Flux and Spectral Index Evolution

The flux evolution of this magnetar after the two outbursts was considered in several studies (Woods et al. 1999; Kouveliotou et al. 2003; Mereghetti et al. 2006a; Esposito et al. 2008). Kouveliotou et al. (2003) tried to explain an apparent plateau in the observed flux evolution of the 1998 outburst (between days 400 and 800) using a crustal cooling model (Lyubarsky et al. 2002). However, Mereghetti et al. (2006a) argued that the unabsorbed

---

<sup>5</sup><http://heasarc.gsfc.nasa.gov/docs/xandau/xspec>

flux does not show a plateau and claimed that the data out to 1000 days were fitted by a power-law decay with index of 0.6 ( $F(t) \propto (t - t_0)^{-0.6}$ ). Esposito et al. (2008) explained the flux decay of the 2008 outburst (for  $\sim 1$  month from the outburst) with a steep phase and a shallow phase.

We show the flux evolution curves including our measurements and previous ones from Mereghetti et al. (2006a) and Esposito et al. (2008, 2009a,b) and show them in Figure 1. We tried to fit the data out to  $\sim 3000$  days with a power law ( $F(t) = F_1(t - t_0)^{-\alpha}$ ; adding a constant quiescent flux did not improve the fit) or an exponential ( $F(t) = F_1 e^{-(t-t_0)/\tau_1} + F_Q$ ) or a double exponential ( $F(t) = F_1 e^{-(t-t_0)/\tau_1} + F_2 e^{-(t-t_0)/\tau_2} + F_Q$ ), but did not obtain a satisfactory fit (reduced  $\chi^2$  of 8.3, 3.0 and 3.9, respectively) for the 1998 outburst. Also a single power law does not describe the flux evolution after the 1998 outburst when we include all the data out to 10 years.

We did not obtain a good fit for the flux evolution of the 2008 outburst with a single component fit. However, the data are well fit by a double exponential with decay constants of  $0.5 \pm 0.1$  and  $59 \pm 6$  days (reduced  $\chi^2=0.7$ ). The fit results are summarized in Table 2. This relaxation trend after the 2008 outburst is similar to what has been observed for other magnetars (e.g. Woods et al. 2004; Rea et al. 2009; Gavril et al. 2008; Livingstone et al. 2011). Note that the individual *Swift* XRT observations (which were in PC mode) after the 2008 outburst did not have enough counts for a meaningful spectral analysis, and thus all the observations were assumed to have identical spectra in determining the fluxes plotted in Figure 1 (Esposito et al. 2008). If the spectral index changed significantly over the first 30 days as seen in other magnetars (e.g. Zhu et al. 2008), the flux values in Figure 1 would have changed too, but only marginally for reasonable assumptions<sup>6</sup>.

We also plot the spectral index evolution curves for the same data in Figure 2, in order to look for a correlation between spectral hardness and flux, as seen in other magnetars (Rea et al. 2005; Woods et al. 2007; Campana et al. 2007; Tam et al. 2008; Zhu et al. 2008; Scholz & Kaspi 2011). It seems that there is no such correlation in this magnetar in the 1998 outburst and only marginal evidence for it in the 2008 outburst. Also, the source spectrum was significantly softer just after the outburst in 1998 than in 2008. To see if there is any bias in spectral parameters caused by the large point spread function (PSF) of *BeppoSAX* and *ASCA* ( $> 2'$ ), using 4 *Chandra* observations (ID: 1981, 3877, 12528, 12529), we looked for any strong soft source that could have affected the low-energy flux in the

---

<sup>6</sup>If we assume the same  $\Gamma$  vs  $L_X$  relation as  $\Delta\Gamma \simeq 0.1\Delta F_x$  ( $10^{-11}$  erg cm<sup>-2</sup> s<sup>-1</sup>) (Zhu et al. 2008), we expect the first *Swift* data point to go down by  $\sim 10\%$  and the rest to go up by  $\sim 10\%$ , making  $\tau_1 = 0.6 \pm 0.1$  and  $\tau_2 = 58 \pm 6$  days.

*BeppoSAX* and *ASCA* observations. However, we find no appropriate source in a radius of  $2'$ . We also checked cross calibration results of different X-ray satellites done with Crab Nebula observations (Kirsch et al. 2005) but the difference in spectral indices as reported by different instruments for SGR 1627–41 appears too large to be due to instrument calibration issues alone.

## 4. Discussion

We have measured the spectrum and flux of SGR 1627–41 three years after its 2008 outburst and find them to be consistent with those measured at the same interval following the 1998 outburst. We also compile the fluxes measured at different times after the two outbursts. The cooling curve after the 2008 outburst is well fitted by a double exponential, while we do not obtain an acceptable fit to the cooling curve after the 1998 outburst. We find at most marginal evidence for a hardness/flux correlation following either outburst.

### 4.1. Flux and Spectral Index Evolution

The flux we measured for SGR 1627–41 in 2011 June is marginally higher (by  $1.5\sigma$ ) compared to the lowest flux previously measured for this magnetar, suggesting that at this flux, the source is near or at quiescence. However, if we compare the spectrum in 2011 to those of other magnetars having low quiescent luminosities, we find that SGR 1627–41 is significantly harder (e.g. XTE J1810–197, 1E 1547.0–5408, Gotthelf et al. 2004; Gelfand & Gaensler 2007). This may be because SGR 1627–41 has not yet reached quiescence. It is also possible that the source has a significant hard X-ray component above  $\sim 10$  keV as observed in other magnetars (Kuiper et al. 2006); such a hard X-ray component could bias the soft X-ray spectrum. Indeed, the source spectrum becomes softer (larger photon index) as we lower the high energy bound of the spectral fit, although the result is not statistically significant due to large uncertainties. It will be interesting to continue to monitor the source’s flux and spectrum to see if the flux drops even lower and to see if the spectrum becomes softer. Also observing the source with future hard X-ray observatories such as *NuSTAR* (Harrison et al. 2010) can help us to determine the hard spectral component above  $\sim 10$  keV, although it may be difficult if the source becomes fainter.

Comparing the flux and spectral evolution after the outburst, we note that at  $\sim 100$  days after the 2008 outburst, the flux was an order of magnitude lower than at the same time after the 1998 outburst, although they became similar after  $\sim 1000$  days. Thus, the

functional forms of the flux decays differ, as do the spectral evolutions (see Figs. 1 and 2). This suggests that some aspects of the mechanism of the 2008 outbursts and/or the flux decay may have been different from that of the 1998 outburst.

Thompson et al. (2002) suggest two different mechanisms for magnetar outbursts. One is a sudden change in the internal magnetic field, causing a fracture of the crust, and the other is a sudden relaxation of the external fields. The X-ray spectrum gets harder immediately after the burst activity in the former case as the fracture will shear magnetic fields, generating more currents and thus more resonant up-scattering in the magnetosphere, while the spectrum gets softer in the latter case as the twist of external magnetic fields is relaxed. More detailed studies have been conducted by Perna & Pons (2011) for the crustal effect and by Lyutikov (2003) for the magnetospheric effect, where the former studied the evolution of magnetic stresses in the crust to calculate properties of outbursts such as energy distribution, outburst waiting time and location of starquakes, and the latter estimated the time scale of explosive magnetospheric reconnection events that can cause magnetar outbursts.

The lack of measurements for the pre-burst spectrum of SGR 1627–41 makes it difficult to diagnose the nature of the 1998 outburst in the magnetar model, as it is not known whether the spectrum was softer or harder before the outburst. However, the pre-burst spectrum was measured for the 2008 outburst and was significantly softer than immediately after the outburst. Thus, the 2008 outburst was likely initiated by a crustal fracture which twisted the external magnetic fields.

Flux evolutions after outbursts may be explained by the untwisting magnetic field model (Beloborodov & Thompson 2007; Beloborodov 2009) and/or the crustal cooling model (e.g. Lyubarsky et al. 2002). Beloborodov (2009) explains that sudden crustal motion can twist the magnetic field and eject currents into the magnetosphere. The currents are then gradually drawn into the star and the magnetic fields are untwisted. The energy is dissipated by Ohmic processes in current-carrying field lines and a large fraction of the power may be radiated at the footpoints of the current. This process can be strongly non-uniform and produce complicated flux evolutions. An example of a cooling curve in the case of a localized starquake (ring-twist) is shown in Figure 10 of Beloborodov (2009).

A different model by Lyubarsky et al. (2002) explains the evolution as an afterglow of the crustal heating. Kouveliotou et al. (2003) explained the observed flux evolution of SGR 1627–41 after its 1998 outburst based on this model with the assumption of a heated inner crust and cool core, which is characterized by a three-phase flux decay: a fast decay followed by a plateau and another rapid decay. However, Mereghetti et al. (2006a) reported that the absorption-corrected flux evolution after the 1998 outburst did not have the plateau which is a characteristic of inner crustal cooling (due to the large heat capacity of the inner



crust), and we agree. Although we do not observe a plateau in the 1998 data, we note that there might be one missed in the 1998 data before  $\sim 50$  days, which is different from the one that Kouveliotou et al. (2003) claimed. In this case, their model may fit the data, but with a different set of parameters. On the other hand, we do seem to observe a three-phase decay following the 2008 event.

In Figure 3, we compare the 2–10 keV luminosity decays following the 1998 and 2008 outbursts with models of crust cooling. To calculate the cooling curves, we follow the thermal evolution of the crust after a rapid deposition of energy at the start of the outburst (see Scholz et al. 2012, for a recent application to Swift J1822–1606). We do this by solving the thermal diffusion equation with a method similar to that used by Brown & Cumming (2009) to model cooling of transiently accreting neutron stars, but with updated microphysics (Cumming et al. 2012, in preparation) to account for the effect of the strong magnetic field on the thermal conductivity (Potekhin 1999) and using a  $T_{\text{eff}}-T_{\text{int}}$  relation for a magnetized envelope (Potekhin & Yakovlev 2001). We include both phonon and impurity scattering in the electron thermal conductivity, and in particular set the impurity parameter  $Q_{\text{imp}} = 3$ . We take the neutron star mass and radius to be  $M = 1.3 M_{\odot}$  and  $R = 12$  km, and take the magnetic field strength to be  $2 \times 10^{14}$  G as inferred from the spin down.

Our calculations are in 1D, but we take into account the effect of the magnetic field on the transport of heat by assuming a dipole geometry for the magnetic field and taking an average over spherical shells (following Potekhin & Yakovlev 2001, based on the approach of Greenstein & Hartke 1983). This means that in our calculation, we assume that the heating occurs in a shell over the entire surface of the star. In reality, the heating is likely localized on the stellar surface, which would reduce the overall luminosity because of the smaller emitting area. This should not change the shape of the cooling curve significantly since the thermal time to the surface in the thin crust is much shorter than the timescale for lateral transport of heat.

We attempt to match the observed cooling curves by choosing the amount of energy deposited in the crust, its location in the crust, and the neutron star core temperature  $T_c$ . The dependence of the energy deposition as a function of depth is not known for magnetar outbursts, and so we adopt the simple approach (following Lyubarsky et al. 2002) of depositing a constant energy density  $E_{25} 10^{25}$  erg cm $^{-3}$  in the crust. For  $B = 2 \times 10^{14}$  G, this represents a fraction  $0.6 E_{25} \%$  of the magnetic energy density. For the 2008 outburst (bottom panel of Fig. 3), we find that heating the crust in the density range  $2 \times 10^9 - 3 \times 10^{10}$  g cm $^{-3}$  with  $E_{25} = 1.4$  matches the shape of the cooling curve well. For the 1998 outburst (top panel of Fig. 3), the energy required is more than ten times larger,  $E_{25} = 16$ , and must be deposited deeper in the crust, at densities  $1 \times 10^{10} - 2 \times 10^{11}$  g cm $^{-3}$  to match the longer decay time

scale.

For the 1998 outburst, while we can match the general shape of the cooling curve, we cannot reproduce both the rapid drop at  $t \approx 1000$  days and the subsequent leveling off of the decay at  $t > 1000$  days with our crust models. This agrees with the conclusions of Kouveliotou et al. (2003), who proposed that the rapid drop was a consequence of a cold core in SGR 1627–41. They found that for a core temperature  $T_c \sim 2 \times 10^7$  K, for example as would be expected if direct URCA neutrino emission operated in the core, the inner crust would cool rapidly by conduction of heat into the core, leading to the observed rapid drop in luminosity at  $t \approx 1000$  days. However, the luminosity we measure in this paper at more than 1000 days following the 2008 outburst requires a neutron star core temperature of  $T_c \approx 2 \times 10^8$  K if it is due to thermal emission from the neutron star surface, and so the 2008 outburst is not consistent with a cold core. For example, we show models with  $T_c = 3 \times 10^7$  K in Figure 3, illustrating that the cooling occurs much too rapidly to explain the observed luminosity. The observed flux at 1000 days is much greater than expected for the cold core case.

Our model predicts that the current source flux will not decline by more than an order of magnitude in a time scale of years. However, we note that the source may not be in the quiescent state yet; the flux may decline slightly to the level of the last data point after the 1998 outburst. In this case, our model will require a slightly lower core temperature ( $\sim 1.5 \times 10^8$  K).

A hardness/flux correlation is expected in magnetar models (Thompson et al. 2002; Lyutikov & Gavriil 2006; Özel & Güver 2007) and has been seen in other magnetars (e.g. Gavriil et al. 2008; Rea et al. 2009; Livingstone et al. 2011). It does not, however, seem to exist clearly in the two outbursts of SGR 1627–41, as seen in Figure 2. This is somewhat unexpected in the magnetospheric untwisting model; an increase in the plasma density and speed after an outburst is expected following a twist of magnetic fields due to a fracture, which decreases as the magnetar relaxes by untwisting the fields. The increase in plasma increases the up-scattering probability, hence resulting in a harder spectrum, with accompanying higher flux due to heat release from the interior event. We note that SGR 1627–41 is not the only magnetar that does not show the correlation. For example, in SGR 1900+14, after its 1998 giant flare, the flux decreased by a factor of three in  $\sim 18$  months while neither the spectral index nor the blackbody temperature changed significantly (Tiengo et al. 2007).

In our crustal cooling model, as the flux declines, a decrease of temperature is nominally expected so the absence of a hardness/flux correlation is also puzzling. However, the degree of discrepancy is unclear as presently our model is not capable of predicting spectral hardness evolution quantitatively. Also, we note that changes in the spectral hardness of the source

(essentially  $kT$  for a crustal cooling event) may not be well represented by the power-law photon index. A better measure might be the blackbody temperature or the soft to hard band flux ratio. However, it was difficult to measure the spectrum unambiguously (especially in the soft band) for this magnetar due to its high absorption and its low count rate.

#### 4.2. Correlation between magnetic field and quiescent luminosity

The quiescent luminosity of this magnetar is the lowest among SGRs as reported by Mereghetti et al. (2006a). However, there are only four SGRs whose distance, hence luminosity, is known approximately. Given that SGRs and AXPs have similar natures, it is interesting to compare the luminosity of SGR 1627–41 with those of other magnetars for which the quantity is relatively well determined and to search for a correlation with, e.g., inferred surface dipolar magnetic-field strength. A correlation between  $B$  and  $L_X$  of magnetars might be expected (Thompson et al. 2002; Pons et al. 2007; Perna & Pons 2011) because, at least for sources of comparable age, a higher  $B$  implies greater internal heating as well as stronger field twisting in the magnetosphere.

To investigate a possible correlation between the spin-inferred surface magnetic field and quiescent luminosity in the X-ray band ( $L_X$ , 2–10 keV) of magnetars, we select magnetars with a reasonable distance estimate from the McGill online magnetar catalog. We take the flux and distance values from references in the catalog. However, for sources that have a two-component spectrum, it was not possible to obtain 2–10 keV flux unless flux normalizations are given in the references. In these cases, we re-analyzed the archival data to obtain the source flux in the 2–10 keV band. To ensure that the luminosity is in quiescence, we verified that the measurement was done long before/after the activity of the magnetar. The data are shown in Table 3 and plotted in Figure 4.

A possible trend between  $B$  and  $L_X$  of magnetars is apparent in Figure 4. To see if the trend is significant, we calculate Pearson’s correlation coefficient ( $r$ , calculated in log-log scale) and Spearman’s rank order correlation coefficient ( $r_s$ ). With the magnetars only (including two candidates), we obtain  $r = 0.63$  ( $r_s = 0.72$ ) with a sample size of  $N = 16$ , corresponding to a null-hypothesis probability of  $p \simeq 0.004$  ( $p \simeq 0.001$  for  $r_s$ , 1-sided). These values suggest a real correlation. However, in neither test are the uncertainties on the values taken into account.

In order to see the effect of uncertainties in the magnetic fields and the luminosities, we performed simulations. We assumed that the uncertainties are 50% for the magnetic-field strength, the flux and the distance, and further assumed a uniform distribution for

the uncertainties. With 10000 simulations, we counted the occurrences in which the null hypothesis could not be rejected ( $p > 0.05$ ). This occurred 200/10000 (480/10000 for  $r_s$ ) times with the magnetars (with the two candidates). Although we cannot formally reject the null hypothesis, this at least suggests a trend between  $B$  and the quiescent luminosity.

For sources that have significant flux below  $\sim 2$  keV, considering the 2–10 keV band only may not be optimal. Therefore, we have repeated this analysis for luminosities in the 1–4 keV range, where thermal emission dominates but where the effects of interstellar absorption are more pronounced, and found similar results to those in the 2–10 keV band.

Note that we have not included upper limit measurements in Table 3 and Figure 4 because of the difficulty of handling them statistically in the correlation calculation and translating the limit to the 2–10 keV band. However, we have verified that in no case is a reported upper limit in clear contradiction with the observed possible trend. An important source to include in the future is SGR 0418+5729, as it has very low reported field with no quiescent X-ray luminosity measured yet, although Turolla et al. (2011) suggest it may have higher-order multipoles, and thus may not lie on the trend at the spin-inferred  $B$ .

On Figure 4, we plot  $L_X \propto B^{4.4}$ , similar to the relation predicted by Thompson & Duncan (1996) from internal heating due to magnetic dissipation. This relation is broadly consistent with the data, albeit considerable scatter exists. Note that the lack of magnetars with  $L_X$  greater than  $10^{36}$  erg s $^{-1}$  is consistent with the internal heating model where the X-ray luminosity saturates at  $L_X = 10^{35}$ – $10^{36}$  erg s $^{-1}$  due to rapid neutrino cooling (van Riper et al. 1991; Thompson & Duncan 1993, 1996). This model, however, explains the quiescent X-ray flux as being thermal in origin, and thus naively would predict a correlation between the quiescent surface temperature and the magnetic field while there is no clear observational correlation between them in the magnetar population (Zhu et al. 2009; Kaspi & Boydstun 2010). This suggests that there can be a significant “twisted magnetospheric” effect in the soft X-ray emission. The “twisted magnetospheric” model (Thompson et al. 2002) predicts a correlation between  $B$  and  $L_X$ , where no simple relation is given due to the difficulty in estimating the “twist” ( $B_\phi/B_\theta$ ). Nevertheless, Thompson et al. (2002) explain that the initial output of a magnetar is provided by surface heating ( $L_X \propto B^{4.4}$ ) and is increased by a modest factor due to multiple scattering. Therefore,  $L_X$  should be a strong function of  $B$  in this model.

Alternatively, Pons et al. (2007, 2009) showed an interesting trend between the effective surface temperature and the magnetic field with 27 neutron stars, including both RPPs and magnetars, over magnetic-field range  $10^{12}$ – $10^{15}$  G. They explain the trend with the decay of crustal currents, where  $T_{eff} \propto B^{1/2}$  is expected in a simple illustrative calculation. If we assume that the luminosity is from blackbody emission (i.e. that the initial output of

magnetars is thermal), we expect  $L \propto B^2$  in this model, which can also roughly describe the possible trend we find (see Fig. 4). On the other hand, pure blackbody emission is likely an oversimplification so more detailed modelling, such as consideration of the effects of an atmosphere, is warranted. Age is also an important factor in determining the luminosity in this model and likely for understanding the scatter in Figure 4.

### 4.3. Connection to High- $B$ RPPs

The 2006 outburst of the young, high- $B$  RPP PSR J1846–0258 (Gavriil et al. 2008) clearly demonstrates a connection between magnetars and high- $B$  RPPs. Also, a model of magneto-thermal evolution in neutron stars (Pons et al. 2007; Perna & Pons 2011), motivated by the apparent correlation between the inferred magnetic field and surface temperature over a broad range of magnetic fields, suggested a connection (see Kaspi 2010, for review). It is interesting to ask if a correlation between  $B$  and  $L_X$  exists in the high- $B$  RPP population, and to search for a connection to the magnetar population.

Using Olausen et al. (2010) and other references (e.g. Zhu et al. 2011; Kaplan & van Kerkwijk 2011), we plot  $B$  vs  $L_X$  of high- $B$  RPPs in Figure 4. Interestingly, we note that these appear roughly consistent with the possible trend noted for magnetars alone. We consider this trend more quantitatively. With high- $B$  RPPs only, we obtain  $r = 0.18$  ( $r_s = 0.1$ ), consistent with the null-hypothesis as one can easily see in the plot. This is not surprising, considering the sample size ( $N = 5$ ) and uncertainties. Also note that the luminosities (2–10 keV) of some high- $B$  RPPs are highly uncertain, as they were measured in a lower energy band (e.g. Kaspi & McLaughlin 2005) and extrapolated to the 2–10 keV band. However, if we combine high- $B$  RPPs and magnetars, we obtain a better correlation of  $r = 0.77$  ( $r_s = 0.82$ ) and  $p < 0.0001$  ( $p < 0.0005$  for  $r_s$ ,  $N = 21$ ) than we do with magnetars alone. Also our simulations to investigate the effect of uncertainties (see Section 4.2) show that the null hypothesis is always rejected in this case. Repeating this analysis in the 1–4 keV band yields similar results. Having a better correlation with high- $B$  RPPs and magnetars than with magnetars alone may suggest that high- $B$  RPPs and magnetars share similar physical processes, which evolve continuously as a function of magnetic field.

There is large scatter in the correlation plot. Uncertainties in estimating the true magnetic field from the inferred surface dipolar magnetic field<sup>7</sup>, distance, unabsorbed flux and age effects are obviously possible contributors. Further, some variation is expected depending

---

<sup>7</sup>Note that some magnetars such as SGR 1900+14 and SGR 1806–20 have a large uncertainty in the spin-down inferred magnetic-field strength due to spin-down rate variations.

on the efficiency of multiple scattering of thermal photons, and radiation localization effects may play a role. However, AXP 4U 0142+61 and 1E 2259+586 stand out as having large luminosities with relatively weak magnetic fields. One possible explanation is that the spin-down inferred magnetic field is sensitive to the dipolar component only and these magnetars have very strong toroidal or multipole components (Thompson et al. 2002; Perna & Pons 2011). X-ray polarimetric observations may be able to test this idea.

## 5. Conclusions

Using *Chandra* observations, we have measured the spectrum and absorbed flux in the 2–10 keV band for SGR 1627–41 approximately 3 years after its 2008 outburst. The spectrum was consistent with a power law having  $\Gamma = 2.9 \pm 0.8$  (or a blackbody having  $kT = 0.85^{+0.25}_{-0.16}$  keV), and the absorbed flux was  $1.0^{+0.3}_{-0.2} \times 10^{-13}$  erg cm $^{-2}$  s $^{-1}$  ( $0.75^{+0.20}_{-0.17} \times 10^{-13}$  erg cm $^{-2}$  s $^{-1}$  for a blackbody spectrum) in 2011 June. Although the source flux is similar to that detected a comparable amount of time following its 1998 outburst and is similar to the lowest yet seen from this source, it is unclear whether it has reached true quiescence, as its spectrum is significantly harder than in other magnetars in quiescence. We showed that the flux evolution of the source after its outburst activity in 2008 followed a double exponential with decay times of  $0.5 \pm 0.1$  and  $59 \pm 6$  days. Our model fitting, assuming the flux relaxation is due to crustal cooling, suggests that the core temperature of SGR 1627–41 is high ( $T_c \sim 2 \times 10^8$  K) and that the energy was deposited in the outer crust (at different depths) for the two outbursts. This is the same conclusion as for Swift J1822–1606 (Scholz et al. 2012) and may provide an interesting constraint on crust breaking models. We show that the 2008 activity of SGR 1627–41 was likely to have been initiated by a crustal fracture, causing a twist of the external magnetic fields. However, for this magnetar, we see no clear correlation between flux and spectral hardness as seen in other magnetars, which is puzzling. Finally, we find a possible correlation between the inferred magnetic field and the quiescent luminosity of 16 magnetars (including two candidates). We also note that the correlation becomes stronger if we include high- $B$  RPPs, which further suggests a connection between high- $B$  RPPs and magnetars. The discovery and detailed study of more high- $B$  RPPs and magnetars in the future will help us to better understand the physical connection between these two populations.

VMK acknowledges support from a Killam Fellowship, an NSERC Discovery Grant, the FQRNT Centre de Recherche Astrophysique du Québec, an R. Howard Webster Foundation Fellowship from the Canadian Institute for Advanced Research (CIFAR), the Canada Research Chairs Program and the Lorne Trottier Chair in Astrophysics and Cosmology. JAT,

AB, EG, and FR acknowledge partial support from NASA through *Chandra* Award Number GO1-12068A issued by the *Chandra* X-ray Observatory Center, which is operated by the Smithsonian Astrophysical Observatory under NASA contract NAS8-03060. AC is supported by an NSERC Discovery Grant and the Canadian Institute for Advanced Research (CIFAR).

## REFERENCES

- Beloborodov, A. M., & Thompson, C. 2007, *ApJ*, 657, 967
- Beloborodov, A. M. 2009, *ApJ*, 703, 1044
- Bernardini, F., Israel, G. L., Dall’Osso, S., Stella, L., Rea, N., Zane, S., Turolla, R., Perna, R., Falanga, M., Campana, S., Götz, D., Mereghetti, S., & Tiengo, A. 2009, *A&A*, 498, 195
- Brown, E. F., & Cumming, A. 2009, *ApJ*, 698, 1020
- Camilo, F., Ransom, S. M., Halpern, J. P., Reynolds, J., Helfand, D. J., Zimmerman, N., & Sarkissian, J. 2006, *Nature*, 442, 892
- Campana, S., Rea, N., Israel, G. L., Turolla, R., & Zane, S. 2007, *A&A*, 463, 1047
- Corbel, S., Chapuis, C., Dame, T. M., & Durouchoux, P. 1999, *ApJ*, 526, L29
- den Hartog, P. R., Kuiper, L., & Hermsen, W. 2008, *A&A*, 489, 263
- Esposito, P., Mereghetti, S., Tiengo, A., Zane, S., Turolla, r., Götz, D., Rea, N., Kawai, N., Ueno, K., Israel, G. L., Stella, L., & Feroci, M. 2007, *A&A*, 476, 321
- Esposito, P., Israel, G. L. , Zane, S., Senziani, F., Starling, R. L. C., Rea, N., Palmer, D. M., Gehrels, N., Tiengo, A., De Luca, A., Götz, D., Merreggetti, S., Romano, P., Sakamoto, T., Barthelmy, S. D., Stella, L., Turolla, R., Feroci, M., & Mangano, V. 2008, *MNRAS*, 390, L34
- Esposito, A., Tiengo, S., Mereghetti, G., Israel, G. L., De Luca, A., Götz, D., Rea, N., Turolla, R., & Zane, S. 2009, *ApJ*, 690, L105
- Esposito, P., Burgay, M., Possenti, A., Turolla, R., Zane, S., De Luca, A., Tiengo, A., Israel, G. L., Mattana, F., Mereghetti, S., Bailes, M., Romano, P., Götz, D., & Rea, N. 2009, *MNRAS*, 399, L44

- Fishman, G. J., et al. 1989, Compton Observatory Science Workshop, ed. W. N. Johnson (NASA Conf. Publ.; Washington, DC: NASA), 2
- Garmire, G. P., Bautz, M. W., Ford, P. G., Nousek, J. A., & Ricker, G. R. 2003, *Proc. SPIE*, 4851, 28
- Gavriil, F. P., Kaspi, V. M., & Woods, P. M. 2002, *Nature*, 419, 142
- Gavriil, F. P., Gonzalez, M. E., Gotthelf, E. V., Kaspi, V. M., Livingstone, M. A., & Woods, P. M. 2008, *Science*, 319, 1802
- Gelfand, J. D., & Gaensler, B. M. 2007, *ApJ*, 667, 1111
- Göhler, E., Wilms, J., & Staubert, R. 2005, *A&A*, 433, 1079
- Gotthelf, E. V., Halpern, J. P., Buxton, M., & Bailyn, C. 2004, *ApJ*, 605, 368
- Greenstein, G., & Hartke, G. J. 1983, *ApJ*, 271, 283
- Harrison, F. A., Boggs, S., Christensen, F., Craig, W., Hailey, C., Stern, D., Zhang, W., Angelini, L., An, H., Bhalereo, V., Brejnholt, N., Cominsky, L., Cook, W. R., Doll, M., Giommi, P., Grefenstette, B., Hornstrup, A., Kaspi, V. M., Kim, Y., Kitaguchi, T., Koglin, J., Liebe, C. C., Madejski, G., Madsen, K. K., Mao, P., Meier, D., Miyasaka, H., Mori, K., Perri, M., Pivovarov, M., Puccetti, S., Rana, V., & Zoglauer, A. 2010, *Proc. SPIE*, 7732, 27
- Halpern, J. P., & Gotthelf, E. V. 2010, *ApJ*, 725, 1384
- Hong, J., van Den Berg, M., Schlegel, E. M., Grindlay, J. E., Koenig, X., Laycock, S., & Zhao, P. 2005, *ApJ*, 635, 907
- Hurley, K., Kouveliotou, C., Woods, P., Mazets, E., Golenetskii, S., Frederiks, D. D., Cline, T., & van Paradijs, J. 1999, *ApJ*, 519, L143
- Kaplan, D. L., & van Kerkwijk, M. H. 2011, *ApJ*, 740, L30
- Kaspi, V. M., & McLaughlin, M. A. 2005, *ApJ*, 618, L41
- Kaspi, V. M. 2007, *Ap&SS*, 308, 1
- Kaspi, V. M., & Boydston, K. 2010, *ApJ*, 710, L115
- Kaspi, V. M. 2010, *Proc. Natl Acad Sci.*, 107, 7147



- Kirsch, M. G. F., Briel, U. G., Burrows, D., Campana, S., Cusumano, G., Ebisawa, K., Freyberg, M. J., Guainazzi, M., Haberl, F., Jahoda, K., Kaastra, J., Kretschmar, P., Larsson, S., Lubinski, P., Mori, K., Plucinsky, P., Pollock, A. M. T., Rothschild, R., Sembay, S., Wilms, J., & Yamamoto, M. 2005, *Proc. SPIE*, 5898, 589803
- Kouveliotou, C., Kippen, M., Woods, P., Richardson, G., Connaughton, V., & McCollough, M. 1998, *IAU Circ.* 6944
- Kouveliotou, C., Eichler, D., Woods, P., Lyubarsky, Y., Patel, S. K., Göğüş, E., van Der Kulis, M., Tennant, A., Wachter, S., & Hurley, K. 2003, *ApJ*, 596, L79
- Kuiper, L., Hermsen, W., Den Hartog, P. R., Collmar, W. 2006, *ApJ*, 645, 556
- Kurma, H. S., & Safi-Harb, S., 2010, *ApJ*, 725, L191
- Levin, L., Bailes, M., Bates, S., Ramesh Bhat, N. D., Burgay, M., Burke-Spolaor, S., D’Amico, N., Johnston, S., Keith, M., Kramer, M., Milia, S., Possenti, A., Rea, N., Stappers, B., & van Straten, W. 2010, *ApJ*, 721, L33
- Livingstone, M. A., Scholz, P., Kaspi, V. M., Ng, C.-Y., & Gavril, F. P. 2011, *ApJ*, 743, L38
- Lyubarsky, Y., Eichler, D., & Thompson, C. 2002, *ApJ*, 580, L69
- Lyutikov, M. 2003, *MNRAS*, 346, 540
- Lyutikov, M., & Gavril, F. P. 2006, *MNRAS*, 368, 690
- McLaughlin, M. A., Rea, N., Gaensler, B. M., Chatterjee, S., Camilo, F., Kramer, M., Lorimer, D. R., Lyne, A. G., Israel, G. L., & Possenti, A. 2007, *A&A*, 670, 1307
- Mereghetti, S., Esposito, P., Tiengo, A., Turolla, R., Zane, S., Stella, L., Israel, G. L., Feroci, M., & Treves, A. 2006, *A&A*, 450, 759
- Mereghetti, S., Esposito, P., Tiengo, A., Zane, S., Turolla, R., Stella, L., Israel, G. L., Götz, D., & Feroci, M., 2006, *ApJ*, 653, 1423
- Mereghetti, S. 2008, *A&A Rev.*, 15, 255
- Muno, M. P., Gaensler, B. M., Clark, J. S., de Grijs, R., Pooley, D., Stevens, I. R., & Portegies Zwart, S. F. 2007, *MNRAS*, 378, L44
- Olausen, S. A., Kaspi, V. M., Lyne, A. G., & Kramer, M., 2010, *ApJ*, 725, 985

- Özel, F., & Güver, T. 2007, *ApJ*, 659, L141
- Perna, R., & Pons, J. A. 2011, *ApJ*, 727, L51
- Pons, J. A., Link, B., Miralles, J. A., & Geppert, U., 2007, *Phys. Rev. Lett.*, 98(7), 071101+
- Pons, J. A., Miralles, J. A., & Geppert, U., 2009, *A&A*, 496, 207
- Potekhin, A. Y. 1999, *A&A*, 351, 787
- Potekhin, A. Y., & Yakovlev, D. G. 2001, *A&A*, 374, 213
- Ng, C. Y., & Kaspi, V. M., 2011, in *AIP Conf. Proc.* 1379, *Astrophysics of Neutron Stars 2010: A Conference in Honor of M. Ali Alpar*, ed. E. Göğüş, T. Belloni & Ü. Ertan (Melville, NY: AIP), 60
- Rea, N., Oosterbroek, T., Zane, S., Turolla, R., Méndez, M., Israel, G. L., Stella, L., & Haberl, F. 2005, *MNRAS*, 361, 710
- Rea, N., Israel, G. L., Turolla, R., Mereghetti, S., Götz, D., Zane, S., Tiengo, A., Hurley, K., Feroci, M., Still, M., Yershov, V., winkler, C., Perna, R., Bernardini, F., Ubertini, P., Stella, L., Campana, M., van Der Klis, M., & Woods, P. 2009, *MNRAS*, 396, 2419
- Rea, N., Esposito, P., Turolla, R., Israel, G. L., Zane, S., Stella, L., Mereghetti, S., Tiengo, A., Götz, D., Göğüş, E., & Kouvelitou, C. 2010, *Science*, 330, 944
- Rea, N., Esposito, P., 2011, in *High-Energy Emission from Pulsars and their Systems*, ed. D. F. Torres & N. Rea (Berlin: Springer), 247
- Rea, N., Israel, G. L., Esposito, P., Pons, J. A., Camero-Arranz, A., Miganani, R. P., Turolla, R., Zane, S., Burgay, M., Possenti, A., Campana, S., Enoto, T., Gehrels, N., Göğüş, E., Götz, D., Kouvelitou, C., Makishima, K., Mereghetti, S., Oates, S. R., Palmer, D. M., Perna, R., Stella, L., & Tiengo, A. 2012, *ApJ*, submitted
- Safi-Harb, S., & Kurma, H. S., 2008, *ApJ*, 684, 532
- Scholz, P., & Kaspi, V. M., 2011, *ApJ*, 739, 94
- Scholz, P., Ng, C. Y., Livingstone, M., Kaspi, V. M., Cumming, A., & Archibald, R. *ApJ*, submitted
- Tam, C. R., Gavriil, F. P., Dib, R., Kaspi, V. M., Woods, P. M., & Bassa, C. 2008, *ApJ*, 677, 503

- Thompson, C., & Duncan, R. C., 1993, *ApJ*, 408, 194
- Thompson, C., & Duncan, R. C., 1995, *MNRAS*, 275, 255
- Thompson, C., & Duncan, R. C., 1996, *ApJ*, 473, 322
- Thompson, C., Lyutikov, M., & Kulkarni, S. R. 2002, *ApJ*, 574, 332
- Tiengo, A., Esposito, P., Mereghetti, S., Sidoli, L., Götz, D., Feroci, M., Turolla, R., Zane, S., Israel, G. L., Stella, L., & Woods, P. 2007, *Ap&SS*, 308, 33
- Tiengo, A., Esposito, P., & Mereghetti, S. 2008, *ApJ*, 680, L133
- Tiengo, A., Esposito, P., Mereghetti, S., Israel, G. L., Stella, L., Turolla, R., Zane, S., Rea, N., Götz, D., & Feroci, M. 2009, *MNRAS*, 399, L74
- Turolla, R., Zane, S., Pons, J. A., Esposito, P., & Rea, N. 2011, *ApJ*, 740, 105
- van Riper, K. A., Epstein, R. I., & Miller, G. S. 1991, *ApJ*, 381, L47
- Wachter, S., Patel, S. K., Kouveliotou, C., Bouchet, P., Özel, F., Tennant, A. F., Woods, P. M., Hurley, K., Becker, W., & Slane, P. 2004, *ApJ*, 615, 887
- Woods, P. M., Kouveliotou, C., van Paradijs, J., Hurley, K., Kippen, R. M., Finger, M. H., Briggs, M. S., Dieters, S., & Fishman, G. J. 1999, *ApJ*, 519, L139
- Woods, P. M., Kaspi, V. M., Thompson, C., Gavriil, F. P., Marshall, H. L., Chakrabarty, D., Flanagan, K., Heyl, J., & Hernquist, L., 2004, *ApJ*, 605, 378
- Woods, P. M., & Thompson, C. 2006, in *Compact Stellar X-ray Sources*, ed. W. H. G. Levin & M. van der Klis (Cambridge University Press, UK, 2006)
- Woods, P. M., Kouveliotou, C., Finger, M. H., Göğüş, E., Wilson, C. A., Patel, S. K., Hurley, K., & Swank, J. H. 2007, *ApJ*, 654, 470
- Zhu, W., Kaspi, V. M., Dib, R., Woods, P. M., Gavriil, F. P., & Archibald, A. M. 2008, *ApJ*, 686, 520
- Zhu, W., Kaspi, V. M., Gonzalez, M. E., & Lyne, A. G. 2009, *ApJ*, 704, 1321
- Zhu, W. W., Kaspi, V. M., McLaughlin, M. A., Pavlov, G. G., Ng, C. -Y., Manchester, R. N., Gaensler, B. M., & Woods, P. M. 2011, *ApJ*, 734, 44

Table 1: Summary of the spectral fit results for an absorbed power law and an absorbed blackbody with Churazov weighting.

Fit Function	$N_H$ ( $10^{22}$ cm $^{-2}$ )	$\Gamma/kT$ (/keV)	Flux <sup>a</sup> ( $10^{-13}$ erg cm $^{-2}$ s $^{-1}$ )	$\chi^2/\text{DoF}$
Power Law	$10^b$	$2.9 \pm 0.8$	$1.0^{+0.3}_{-0.2}$	12.1/21
Blackbody	$10^b$	$0.85^{+0.25}_{-0.16}$	$0.75^{+0.20}_{-0.17}$	14.5/21

Fits are conducted in the 2–8 keV band. All uncertainties are at the 90% confidence level.

<sup>a</sup>Absorbed flux in the 2–10 keV band.

<sup>b</sup>Frozen at the value from Esposito et al. (2009a).

Table 2: Fit results for the flux evolution after the 2008 outburst.

Fit Function	$F_1^a$ ( $10^{-12}$ erg cm $^{-2}$ s $^{-1}$ )	$\alpha/\tau_1$ (/days)	$F_2^a$ ( $10^{-12}$ erg cm $^{-2}$ s $^{-1}$ )	$\tau_2$ (days)	$F_Q^a$ ( $10^{-12}$ erg cm $^{-2}$ s $^{-1}$ )	$\chi^2/\text{DoF}$
Power Law	7.6(3)	0.60(2)	...	...	...	51/12
Exponential	2.9(2)	48(5)	...	...	0.23(4)	308/11
Double exponential	28(3)	0.5(1)	2.1(2)	59(6)	0.22(4)	6/9

<sup>a</sup>Unabsorbed flux in the 2–10 keV band.

Table 3: Spin-inferred surface magnetic-field strength and 2–10 keV quiescent X-ray luminosity of magnetars and high- $B$  RPPs.<sup>a</sup>

Source Name	$B$ ( $10^{14}$ G)	$F_X^b$ ( $10^{-12}$ erg cm $^{-2}$ s $^{-1}$ )	Distance (kpc)	$L_X^c$ ( $10^{35}$ erg s $^{-1}$ )	Ref.
Swift J1822–1606	0.38	0.04	1.6	$1.2 \times 10^{-4}$	1
1E 2259+586	0.59	17.7	4.0	$3.4 \times 10^{-1}$	2
CXO J164710.2–455216	0.95	0.14	5	$4.2 \times 10^{-3}$	3
4U 0142+61	1.3	70.2	3.6	1.1	4
XTE J1810–197	2.1	0.02	3.5	$3.5 \times 10^{-4}$	5
1E 1547.0–5408	2.2	0.56	3.9	$1.0 \times 10^{-2}$	6
SGR 1627–41	2.2	0.17	11.0	$2.5 \times 10^{-2}$	7
PSR J1622–4950 <sup>d</sup>	2.8	0.065	9	$6.3 \times 10^{-3}$	8
1E 1048.1–5937	3.9	5.8	2.7	$5.0 \times 10^{-2}$	9
CXOU J010043.1–721134	3.9	0.14	60	$6.1 \times 10^{-1}$	10
1RXS J170849.0–400910	4.6	36	8	$6.2 \times 10^{-1}$	11
CXOU J171405.7–381031 <sup>d</sup>	5	3.2	8	$2.4 \times 10^{-1}$	12
SGR 0526–66	5.6	0.48	50	1.4	13
1E 1841–045	6.9	22	8.5	1.9	14
SGR 1900+14	7	4.8	13.5	1.0	15
SGR 1806–20	24	18	8.7	1.6	16
PSR B1916+14	0.16	$2.1 \times 10^{-3}$	2.1	$1.1 \times 10^{-5}$	17
PSR J1119–6127	0.41	$4.7 \times 10^{-2}$	8.4	$3.9 \times 10^{-3}$	18
PSR J1819–1458 <sup>e</sup>	0.5	$1.9 \times 10^{-3}$	3.6	$2.9 \times 10^{-5}$	19
PSR J1734–3333	0.52	$4.3 \times 10^{-3}$	6.1	$1.9 \times 10^{-4}$	20
PSR J1718–3718	0.74	$1.2 \times 10^{-3}$	4.5	$2.9 \times 10^{-5}$	21

See McGill SGR/AXP online catalog and references therein. For pulsar data, see Olausen et al. (2010) and references therein. Refs: [1] (Scholz et al. 2012) [2] (Zhu et al. 2008) [3] (Muno et al. 2007) [4] (Göhler et al. 2005) [5] (Gotthelf et al. 2004) [6] (Gelfand & Gaensler 2007) [7] (Esposito et al. 2008) [8] (Levin et al. 2010) [9] (Tam et al. 2008) [10] (Tiengo et al. 2007) [11] (den Hartog et al. 2008) [12] (Halpern & Gotthelf 2010) [13] (Tiengo et al. 2009) [14] (Kumar & Safi-Harb 2010) [15] (Mereghetti et al. 2006b) [16] (Esposito et al. 2007) [17] (Zhu et al. 2009) [18] (Safi-Harb & Kumar 2008) [19] (McLaughlin et al. 2006) [20] (Olausen et al. 2010) [21] (Zhu et al. 2011)

<sup>a</sup>Upper limit measurements are not included as they cannot be used in the correlation coefficient calculation.

<sup>b</sup>The lowest unabsorbed flux ever measured for the magnetar in the 2–10 keV band. Converted with PIMMS or XSPEC if 2–10 keV unabsorbed flux is not given in the reference.

<sup>c</sup>Calculated from  $F_X$  and distance.

<sup>d</sup>Candidates.

<sup>e</sup>Classified as a rotating radio transient (RRAT).

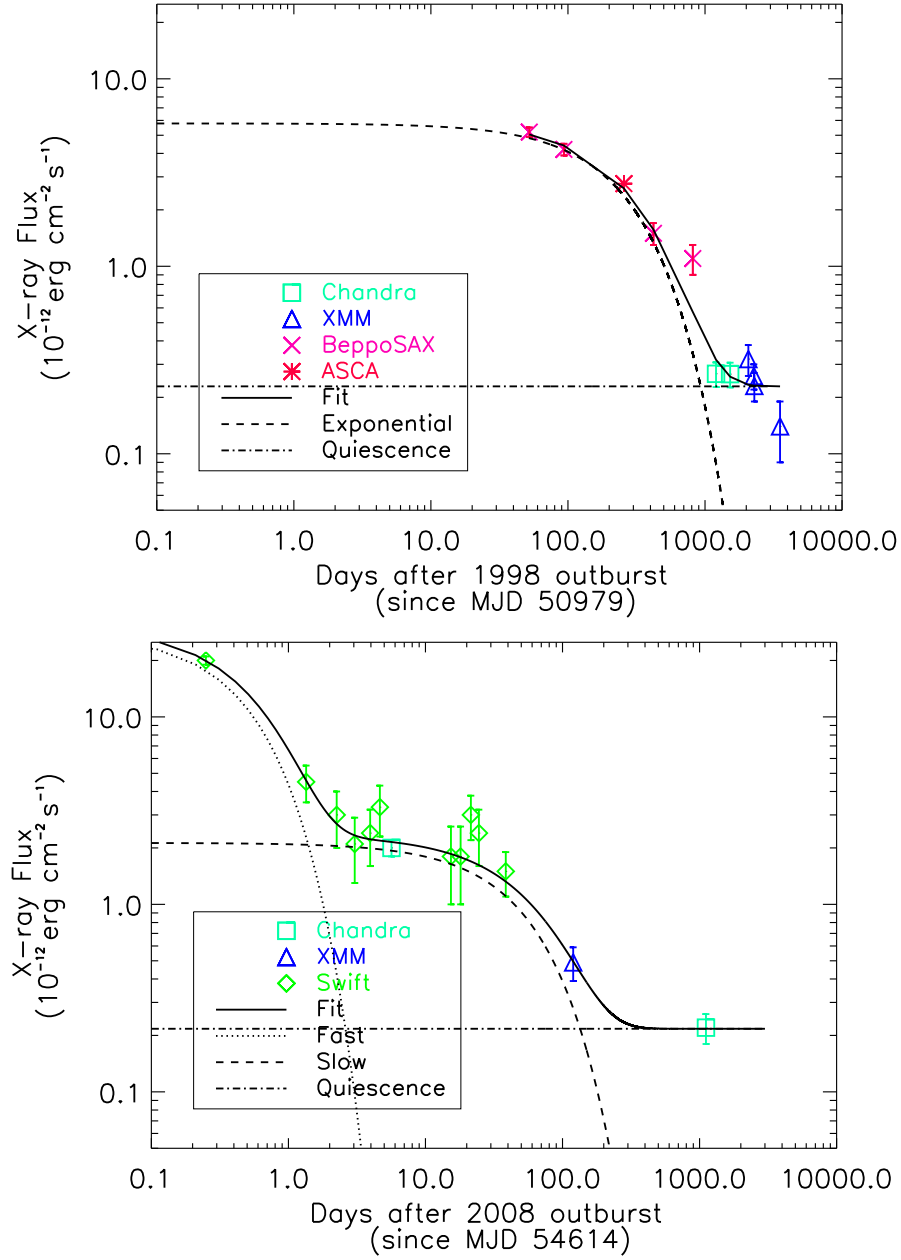


Fig. 1.— 2–10 keV flux values and best-fit function (solid line) for the flux evolution after the 1998 (top) and 2008 (bottom) outbursts. For the 1998 outburst, neither a power law nor an exponential decay gives a satisfactory fit to the flux evolution (an exponential fit is shown in the plot). The 2008 outburst data are well fit by a double exponential with decay constants of 0.5 and 59 days. Data are taken from Mereghetti et al. (2006a), Esposito et al. (2008, 2009a,b) and this work.

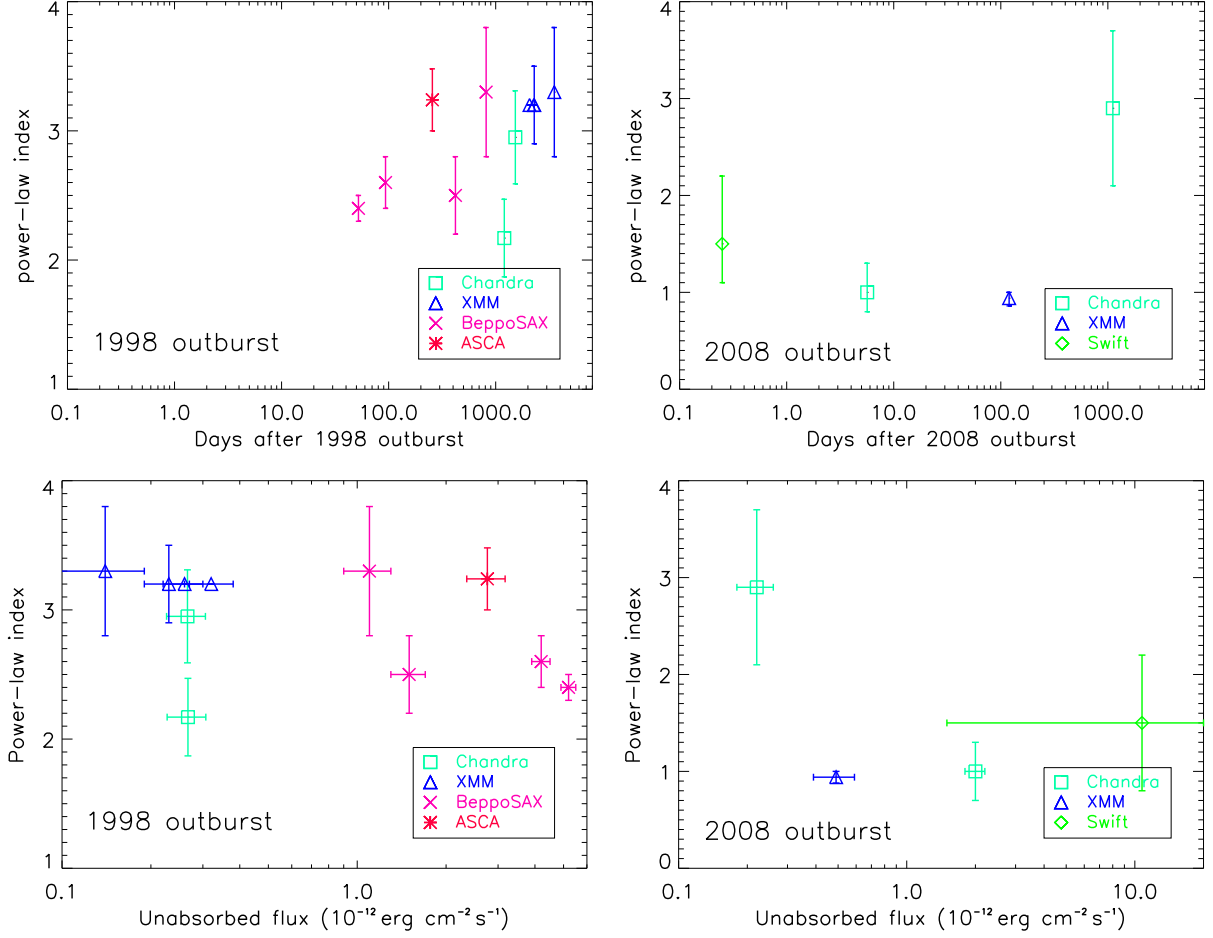


Fig. 2.— Power-law index  $\Gamma$  vs time and 2–10 keV unabsorbed flux for the 1998 and 2008 outburst relaxations.  $\Gamma$  for two *XMM-Newton* data points at  $\sim 2000$  days in the left panels was fixed because of the low counts statistics (Mereghetti et al. 2006a). Due to the low count rate in the *Swift* observations, all the *Swift* data are combined to obtain only one spectral index in the right panels. Data are taken from Mereghetti et al. (2006a), Esposito et al. (2008, 2009a,b) and this work.

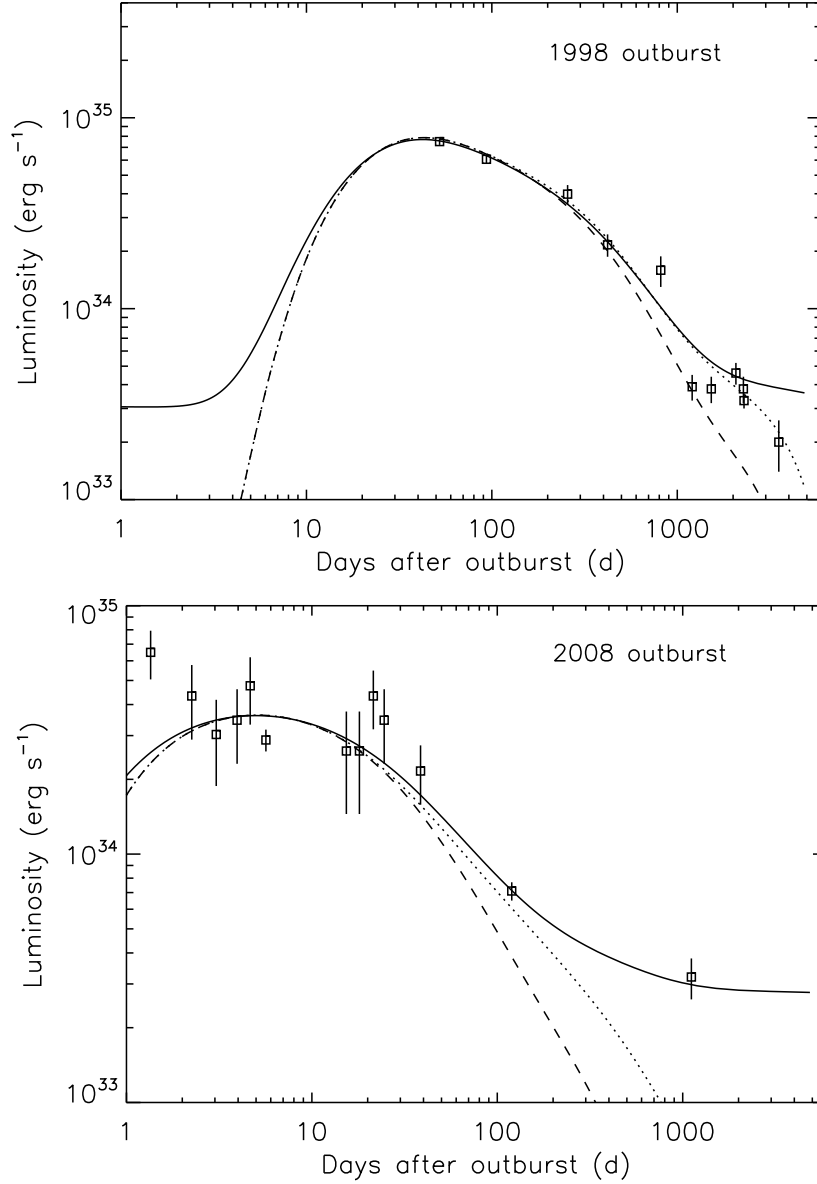


Fig. 3.— Comparison of crust cooling models with the 2–10 keV luminosity decays following the outbursts in 1998 (top panel) and 2008 (bottom panel). All of the models shown assume a constant energy density  $E_{25}10^{25}$  erg cm<sup>-3</sup> is deposited instantaneously in the crust at densities  $\rho_{min} < \rho < \rho_{max}$ . *Top panel* (1998 outburst): The solid curve is for  $1 \times 10^{10} < \rho < 2 \times 10^{11}$  g cm<sup>-3</sup>,  $E_{25} = 16$ ,  $T_c = 2 \times 10^8$  K. The dashed curve is for a cold core,  $1 \times 10^{10} < \rho < 2 \times 10^{11}$  g cm<sup>-3</sup>,  $E_{25} = 18$ ,  $T_c = 3 \times 10^7$  K. The dotted curve is for energy deposition extending to  $1 \times 10^{10}$  g cm<sup>-3</sup>, with  $E_{25} = 18$ ,  $T_c = 3 \times 10^7$  K. *Bottom panel* (2008 outburst): The solid curve is for  $2 \times 10^9 < \rho < 3 \times 10^{10}$  g cm<sup>-3</sup>,  $E_{25} = 1.4$ ,  $T_c = 2 \times 10^8$  K; the dashed curve has  $2 \times 10^9 < \rho < 3 \times 10^{10}$  g cm<sup>-3</sup>,  $E_{25} = 1.7$ ,  $T_c = 3 \times 10^7$  K. The dotted curve is for  $2 \times 10^9 < \rho$ ,  $E_{25} = 1.7$ ,  $T_c = 3 \times 10^7$  K.



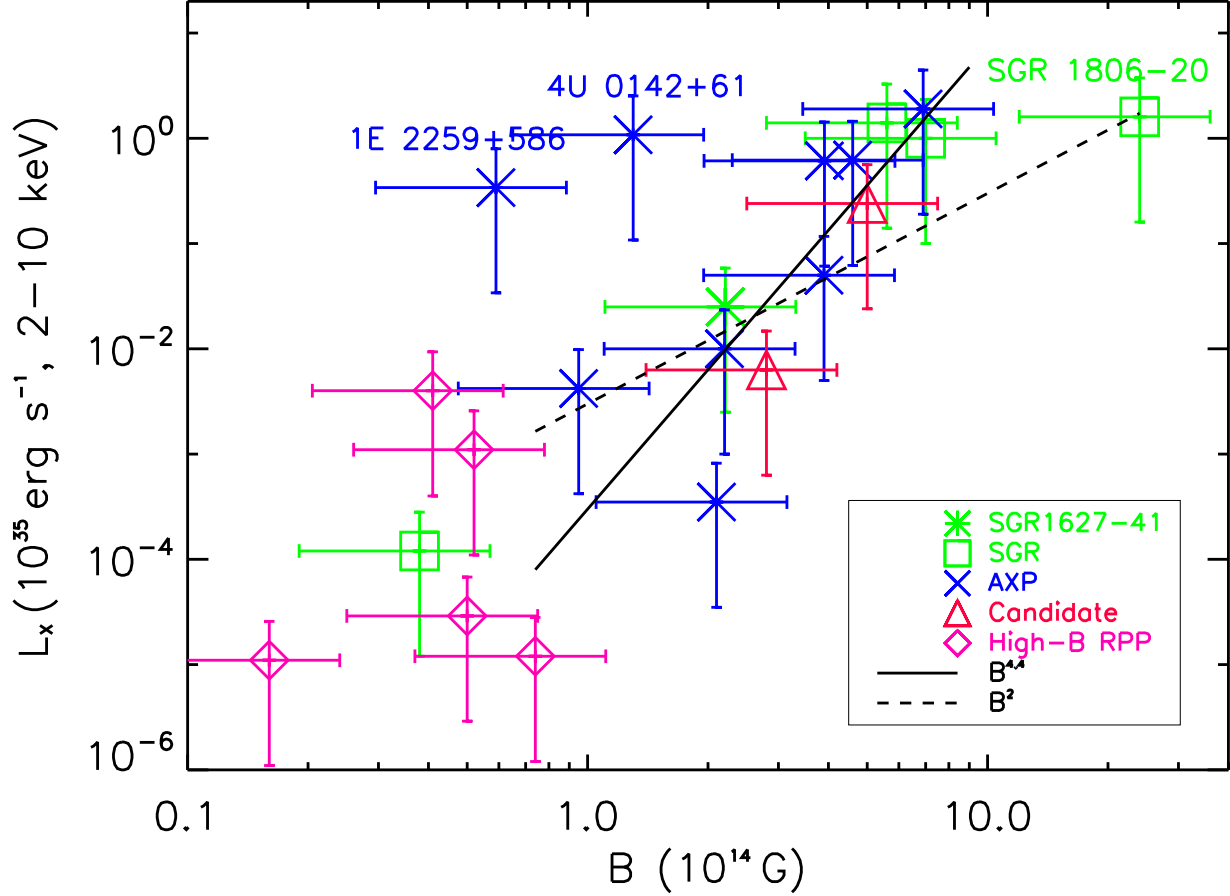


Fig. 4.—  $B$  vs  $L_X$  (2–10 keV) of magnetars and high- $B$  RPPs with known distance including two magnetar candidates (PSR J1622–4950, CXOU J171405.7–381031). See Table 3 for data. The solid line indicates the relation,  $L_X \propto B^{4.4}$ , given by Thompson & Duncan (1996), and the dashed line shows the relation,  $L_X \propto B^2$ , obtained with the  $kT$  vs  $B$  relation of Pons et al. (2007) and an assumption of pure blackbody emission. A possible trend between the surface magnetic-field strength and the luminosity can be seen. Uncertainties of 50% on the distance and the flux are assumed.